American Mineralogist, Volume 97, pages 1256–1259, 2012

LETTER

Graphite in the martian meteorite Allan Hills 84001

ANDREW STEELE,[1,*] FRANCIS M. MCCUBBIN,[2] MARC D. FRIES,[3] D.C. GOLDEN,[4] DOUGLAS W. MING,[5] AND LIANE G. BENNING[6]

[1]Geophysical Laboratory, Carnegie Institution of Washington, 5251 Broad Branch Road, Washington, D.C. 20015, U.S.A.
[2]Institute of Meteoritics, Department of Earth and Planetary Sciences, University of New Mexico, Albuquerque, New Mexico 87131, U.S.A.
[3]Planetary Science Institute, 1700 East Fort Lowell, Suite 106, Tucson, Arizona 85719, U.S.A.
[4]ESCG-Hamilton Sundstrand, Mail Code JE23, Houston, Texas 77058, U.S.A.
[5]Building 31, NASA Johnson Space Center, Clear Lake Houston, Texas 77058, U.S.A.
[6]School of Earth and Environment, University of Leeds, Leeds LS2 9JT, U.K.

ABSTRACT

We use confocal Raman imaging spectroscopy and transmission electron microscopy to study the martian meteorite Allan Hills (ALH) 84001, reported to contain mineral assemblages within carbonate globules (carbonate + magnetite), interpreted as potential relict signatures of ancient martian biota. Models for an abiologic origin for these assemblages required the presence of graphite, and this study is the first report of graphite within ALH 84001. The graphite occurs as hollow spheres (nano-onions), filaments, and highly crystalline particles in intimate association with magnetite in the carbonate globules. In addition to supporting an abiologic origin for the carbonate globule assemblages in ALH 84001, this work proves that there is an inventory of reduced-carbon phases on Mars that has not yet been thoroughly investigated.

Keywords: Martian life, SNC, organic carbon, Mars Science Lab, Raman spectroscopy, magnetite, volatiles

INTRODUCTION

Studies of the martian meteorite Allan Hills (ALH) 84001 have hinted at the presence of reduced-carbon phases (Jull et al. 1998; McKay et al. 1996; Steele et al. 2007). Jull et al. (1998) have shown that a high-temperature, possibly crystalline, carbon phase containing no terrestrial ^{14}C is present in ALH 84001. The nature and provenance of this high-temperature carbon phase has not previously been unambiguously identified. However, Steele et al. (2007) has postulated that the likeliest candidate is a reduced-macromolecular-carbon (MMC) phase that is associated with magnetite in ALH 84001. Furthermore, experimental and theoretical work on the thermal decomposition of siderite (French 1971; French and Rosenberg 1965) has previously been used to postulate a non-biological explanation for the polycyclic-aromatic hydrocarbons and magnetite in this meteorite (McCollom 2003; Steele et al. 2007; Treiman 2003). However, due to the contamination of ALH 84001 by terrestrial organic material, no definitive proof of this process has previously been reported (Brearley 2003; McKay et al. 1996; Steele et al. 2007, 2000; Treiman 2003). In this study we report the unambiguous detection of a range of graphitic carbon morphologies in ALH 84001 both by transmission electron microscopy (TEM) of extracted residue and by in situ mapping of carbonates by confocal Raman imaging spectroscopy (CRIS).

ANALYTICAL METHODS

We collected Raman spectra and images using a Witec α-SNOM, customized to incorporate confocal Raman spectroscopic imaging. The excitation source is a frequency-doubled solid-state YAG laser (532 nm) operating between 0.3 and 1 mW output power (dependent on objective). Objective lenses used included a ×100 LWD and a 20 LWD with a 50 μm optical fiber acting as the confocal pinhole. For the collection of multispectral images, Raman spectra were collected (0–3600 cm^{-1} using the 600 lines mm^{-1} grating) at each pixel using an integration time of between 1 and 6 s per pixel. The effects of interfering peaks were removed by phase masking routines based on multiple single-peak fits that were compared to standardized mineral spectra. Spectral peak identification and methods used in the present study were the same as outlined in Steele et al. (2007). Graphite standards were commercially obtained.

Acid-insoluble graphitic carbon and magnetite particles from harvested chips of the ALH 84001 carbonate globules, which included rim and inner zones, were extracted using 20% (vol/vol) acetic acid at 65–72 °C by a two-step extraction process. The acid extract containing the magnetite and carbon particles was washed 4 times using excess water and micro-centrifugation at 13 900 g for 5 min. Any floating particles on the supernatant were transferred using a Pt loop to the C-substrate of a Cu-grid (Ladd Research Industries). The residue was dispersed in 0.5 mL of water by sonication and deposited on grids. High-resolution imaging was done using a JEOL 2000FX TEM operated at 200 kV, 10 nA beam current (from a LaB6 filament) in the bright-field mode. Randomly distributed nanometer scale domains caused a continuous ring pattern rather than discrete spots. Elemental composition from EDS analyses and lattice spacings from electron diffraction were used to characterize graphite and magnetite. Graphite spacings are indicated in the text and for magnetite the following spacings were used (0.297, 0.253, 0.209, and 0.148 nm).

RESULTS

Figure 1 (spectra i–iv) shows four Raman spectra of MMC/graphitic carbon within carbonate globules of ALH 84001 compared to natural (v) and single-crystal graphite (vi). All these spectra show the characteristic disordered (D) and ordered (G) (labeled in Fig. 1, spectrum i) Raman peaks of MMC/graphitic carbon and, in the case of Figure 1, spectra ii–vi, the characteristic second-order bands (2D) of graphitic carbon. As the grain size of graphitic carbon decreases, crystalline disorder increases, caus-

* E-mail: asteele@ciw.edu

0003-004X/12/0007–1256$05.00/DOI: http://dx.doi.org/10.2138/am.2012.4148

ing the D band to increase in intensity, both the G and D band peak widths to expand, and the 2D bands to decrease in intensity (Fries and Steele 2008; Steele et al. 2007, 2010). Spectrum i in Figure 1 is characteristic of a poorly ordered polycrystalline graphite or completely amorphous carbon, and for convenience has been called macromolecular carbon (MMC) in previous studies (Steele et al. 2007). In Figure 1, spectra ii–v show the spectra from ALH84001 as a function of apparent stacking order; spectrum vi (Fig. 1) is from a single-crystal graphite standard that contains no D band (Ferrari and Robertson 2000; Pimenta et al. 2007). To summarize, Raman data reveal that there is a range of graphite/MMC types in ALH 84001 (Steele et al. 2007). Figures 2a–2e shows a light microscopy image (Fig. 2a) and CRIS maps of carbonate, magnetite, graphite, as well as a combined magnetite-graphite map. Graphite (Figs. 2d and 2e) is associated with magnetite (Figs. 2c and 2e) in the rim and the carbonates. Figure 3 shows the presence of clusters of single-domain magnetite crystals (white arrows in Figs. 3a–3b). Blooms of graphitic carbon can be seen bound to these magnetite crystal clusters, with morphologies varying from amorphous to highly crystalline particles (red arrows in Figs. 3a–3b). Higher magnification TEM imaging of the graphitic carbon reveals complete grains, as well as ribbons and hollow spheres formed by graphite layers (Fig. 4). The graphitic structures were verified by selected-area electron diffraction (Fig. 4b) and *d*-spacing measurements of 3.4 Å, as illustrated by the white arrows in Figure 4e (Daniels et al. 2007). Figure 4d shows that the hollow sphere morphology

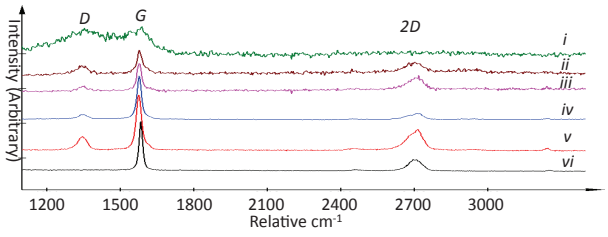

Figure 1. Raman spectra of MMC (i) and graphite from ALH 84001 (ii–iv) as well as natural graphite from Sri Lanka (v) and a single graphite crystal (vi) showing characteristic D and G peaks, as well as the second-order bands of crystalline graphite.

of some of the graphite is reminiscent of mesoporous graphite micro-textures (Kruk et al. 2007; Yang et al. 2004). These spheres appear to consist of polyaromatic platelets surrounding more ordered graphite layers (red and black arrows, respectively, in Fig. 4d) (Yang et al. 2004).

Discussion

The different morphologies of graphite shown by TEM are consistent with the range of D and G peak parameters seen in the Raman spectroscopy data (i.e., Shi et al. 2010; Fig. 1 this study). The appearance/morphology of graphite in ALH 84001 is unusual although similar morphologies have been described in terrestrial systems, meteorites and impact studies (Kovalevski et al. 2001; Buseck et al. 1997; Smith and Buseck 1981; Tan et al. 2010). Such structures have been given a variety of names including: mesoporous graphite, nano-graphite, nano-onions, carbon nanorings, and fulleroids (Kovalevski et al. 2001; Buseck et al. 1997; Smith and Buseck 1981; Tan et al. 2010). Experimentally produced graphite hollow spheres, capsules, and solid graphite particles below 200 nm in diameter have Raman spectra similar to those in Figure 1, spectra i–iv, and in previous studies of ALH 84001 (Ferrari and Robertson 2000; Pimenta et al. 2007; Shi et al. 2010; Steele et al. 2007). Similar mesoporous or fulleroid graphite structures containing large polyaromatic-hydrocarbon "platelet" morphologies have been described as forming from a mixture of organic materials, porous silica, and iron oxide particles (Kruk et al. 2007). Shi et al. (2010) have described a system where a similar combination of graphite morphologies was synthesized from an organic precursor reduced in the presence of Mg. Interestingly, as the temperature of formation decreased from 600 to 400 °C, the morphology of the graphite shifted from solid graphite particles to hollow capsules to hollow spheres (Shi et al. 2010; Talyzin et al. 2009). None of these experimental, meteoritic or terrestrial systems appears specifically applicable to the conditions experienced by ALH 84001. However, the underlying trend of each of these instances is that in all cases high temperatures are required in their formation (Tan et al. 2010; Shi et al. 2010; Kovalevski et al. 2001; Buseck et al. 1997; Smith and Buseck 1981). Figure 4d (red arrow) shows the presence of similar "platelets" of graphene sheets as those

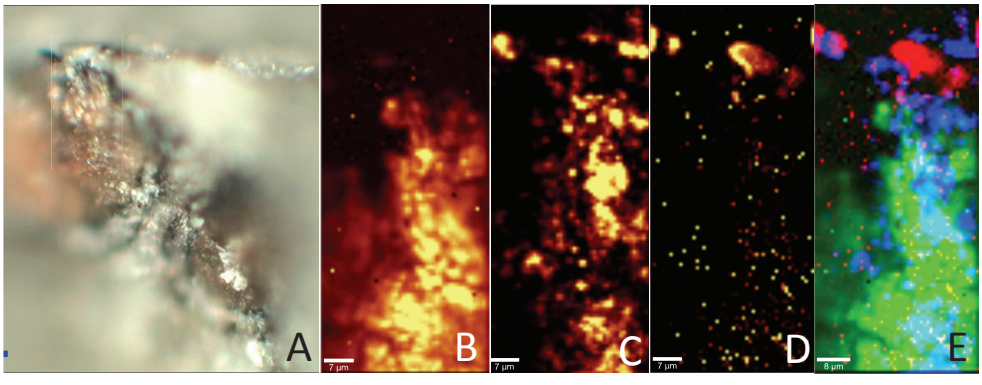

Figure 2. (**a**) Light microscopy image of two carbonate globules from the interior of ALH 84001. (**b**–**d**) CRIS maps of carbonate (1083 cm^{-1}), magnetite (660 cm^{-1}), and graphite G band (1570 cm^{-1}), where a lighter color indicates a more intense signal; (**e**) CRIS Red Green Blue combined maps (from **b**–**d**)—red: graphite, blue: magnetite, green: carbonate—showing spatial relationships in rim of the carbonate globule framed in **a** (scale bars in **b**–**e**: 7 µm).

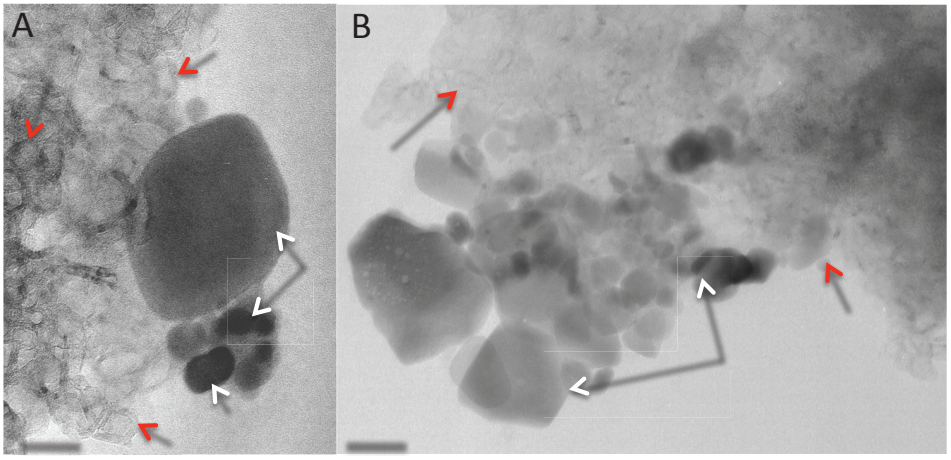

FIGURE 3. (**a**–**b**) TEM images of single-domain magnetite crystals (white arrows) attached to a cloud of graphite spheres and filaments (examples highlighted by red arrows). Scale bars: 20 nm.

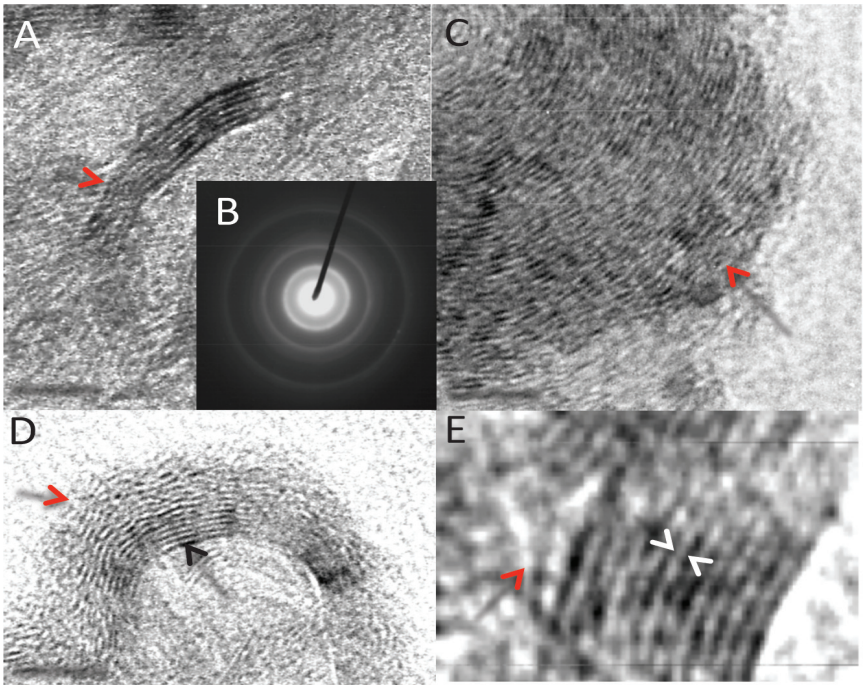

FIGURE 4. High-magnification TEM images of graphite morphologies associated with magnetite seen in Figure 3. (**a**) A hollow graphite capsule showing layering of graphite sheets with inset (**b**), the characteristic SAED pattern of graphite with corresponding *d*-spacings of 3.35 Å (002), 2.05 Å (101), and 1.70 Å (004); (**c**) larger, more ordered graphite particle (red arrow); (**d**) graphite shell resembling nano-rings/onions, with 9–15 ordered hexagonal layers (black arrow) transforming into disordered poly-aromatic platelets at upper edge (red arrow); (**e**) typical graphite *d*-spacing of 3.35 Å (between white arrows); red arrow indicates split graphite sheets to further accommodate graphene layers at fork. Scale bars: in **a**, 20 nm; in **c**, 6 nm; in **d**, 5 nm.

described by Yang et al. (2004). These platelets are essentially polycyclic-aromatic hydrocarbons (PAHs) of varying sizes, and the presence of this class of organic molecule in ALH84001 may also be accounted for by changing conditions during graphite formation (Steele et al. 2007; Yang et al. 2004). The domain size of the platelet shown by the red arrow in Figure 4d is in the size range of that known for coronene (~11.4 Å; Cho et al. 1998), a PAH detected by McKay et al. (1996) in this meteorite.

After the claims of possible relict signatures of martian biota in the carbonate globule assemblages in ALH 84001 (McKay et al. 1996), many looked for an abiotic explanation for the development of the carbonate assemblages. This approach required an understanding of the phase relationships of iron oxides, graphite (which had not been identified), and CO_2 over a range of P, T, and f_{O2} (Brearley 2003; French 1971; French and Rosenberg 1965; Koziol 2004; McCollom 2003; Steele et al. 2007; Treiman et al. 2002; Treiman and Essene 2011). Within these relationships there are two competing abiotic hypotheses to explain the carbonate assemblages, both of which require the presence of graphite: (1) graphite formation during primary growth of the carbonate globules and (2) impact formation from thermal decomposition of the siderite-rich carbonate in already formed globules. In the former hypothesis, as CO_2-containing aqueous fluids cooled out of equilibrium, f_{O2} fluctuated to a large extent at the nanoscale within the growing carbonates. Under these conditions, graphite deposition with magnetite would be possible during the bulk

deposition of carbonate (Brearley 2003; French 1971; French and Rosenberg 1965; Koziol 2004; McCollom 2003; Steele et al. 2007; Treiman et al. 2002; Treiman and Essene 2011). In the latter, the same phase relationships are applicable, but siderite in already formed globules decomposes to graphite and magnetite during a transient heating event possibly linked to impact derived ejection from the martian surface (Brearley 2003; French 1971; French and Rosenberg 1965; Koziol 2004; McCollom 2003; Steele et al. 2007; Treiman et al. 2002; Treiman and Essene 2011). In terrestrial systems, fluid-deposited graphite has been reported as low as 350 °C, coexistent with carbonate at temperatures of 500–600 °C (Luque et al. 1998, 2009; van Zuilen et al. 2003). Similar graphite morphologies have been reported from Shungite rocks formed at over 500 °C (Kovalevski et al. 2001; Buseck et al. 1997; Goodarzi and Murchison 1973). McCollom (2003) synthesized a range of PAHs from the thermal decomposition of siderite and postulated that this mechanism would limit the formation of PAHs in ALH 84001 to between 400 and 600 °C in a post-deposition impact event. If similar temperature conditions as these occurred during the formation of graphite in ALH 84001, then this is in conflict with recent studies showing a low formation temperature (~18 °C) for the carbonate globules that host the graphite (i.e., Halevy et al. 2011). The presence of graphite morphologies that form at higher temperatures indicate that ALH 84001 carbonate globules underwent a transient heating possibly >350 °C, either during formation or due to impact. Importantly, the presence of graphite associated with magnetite in the carbonate assemblages in ALH 84001 lends credence to either of the proposed models for an abiologic origin for those assemblages. Furthermore, this graphite is the first unambiguous account of a reduced-carbon phase indigenous to Mars.

Acknowledgments

This work was financially supported by NASA ASTEP (NNX09AB74G to A.S.), SRLIDAP, MFRP (NNX08AN61G to A.S.), and Cosmochemistry (NNX-11AG76G to F.M.). We acknowledge support from Witec GmbH, and we thank Steve Squyres for useful discussions. We also thank Mark van Zuilen, Bradley De Gregorio, and an anonymous reviewer for their comments.

References cited

Brearley, A.J. (2003) Magnetite in ALH 84001: An origin by shock-induced thermal decomposition of iron carbonate. Meteoritics & Planetary Science, 38, 849–870.

Buseck, P.R., Galdobina, L.P., Kovalevski, V.V., Rozhkova, N.N., Valley, J.W., and Zaidenberg, A.Z. (1997) Shungites: the C-rich rocks of Karelia, Russia. Canadian. Mineralogist, 35, 1363–1378.

Cho, K.A., Shimada, T., Sakurai, M., and Koma, A. (1998) Effect of growth temperature and substrate materials on epitaxial growth of coronene. Journal of Applied Physics, 84, 268–274.

Daniels, H., Brydson, R., Rand, B., and Brown, A. (2007) Investigating carbonization and graphitization using electron energy loss spectroscopy (EELS) in the transmission electron microscope (TEM). Philosophical Magazine, 87, 4073–4092.

Ferrari, A.C. and Robertson, J. (2000) Interpretation of Raman spectra of disordered and amorphous carbon. Physical Review B, 61, 14095–14107.

French, B.M. (1971) Stability relations of siderite ($FeCO_3$) in the system Fe-C-O. American Journal of Science, 271, 37–78.

French, B.M. and Rosenberg, P.E. (1965) Siderite ($FeCO_3$): Thermal decomposition in equilibrium with graphite. Science, 147, 1283–1284.

Fries, M. and Steele, A. (2008) Graphite whiskers in CV3 meteorites. Science, 320, 91–93.

Goodarzi, F. and Murchison, D.G. (1973) Oxidized vitrinites—Their aromaticity, optical properties and possible detection. Fuel, 52, 90–92.

Halevy, I., Fischer, W.W., and Eiler, J.M. (2011) Carbonates in the Martian meteorite Allan Hills 84001 formed at 18 ± 4 degrees C in a near-surface aqueous environment. Proceedings of the National Academy of Sciences, 108, 16895–16899.

Jull, A.J.T., Courtney, C., Jeffrey, D.A., and Beck, J.W. (1998) Isotopic evidence for a terrestrial source of organic compounds found in Martian meteorites Allan Hills 84001 and Elephant Moraine 79001. Science, 279, 366–369.

Kovalevski, V.V., Buseck, P.R., and Cowley, J.M. (2001) Comparison of Carbon in Shungite rocks to other natural carbons: An X-ray and TEM study. Carbon, 39, 243–256.

Koziol, A.M. (2004) Experimental determination of siderite stability and application to Martian Meteorite ALH 84001. American Mineralogist, 89, 294–300.

Kruk, M., Kohlhaas, K.M., Dufour, B., Celer, E.B., Jaroniec, M., Matyjaszewski, K., Ruoff, R.S., and Kowalewski, T. (2007) Partially graphitic, high-surface-area mesoporous carbons from polyacrylonitrile templated by ordered and disordered mesoporous silicas. Microporous and Mesoporous Materials, 102, 178–187.

Luque, F.J., Pasteris, J.D., Wopenka, B., Rodas, M., and Barrenechea, J.F. (1998) Natural fluid deposited graphite: Mineralogical characteristics and mechanisms of formation. American Journal of Science, 298, 471–498.

Luque, F.J., Ortega, L., Barrenechea, J.F., Millward, D., Beyssac, O., and Huizenga, J.-M. (2009) Deposition of highly crystalline graphite from moderate-temperature fluids. Geology, 37, 275–278.

McCollom, T.M. (2003) Formation of meteorite hydrocarbons from thermal decomposition of siderite ($FeCO_3$). Geochimica et Cosmochimica Acta, 67, 311–317.

McKay, D.S., Gibson, E.K., Thomas-Keprta, K.L., Vali, H., Romanek, C.S., Clemett, S.J., Chillier, X.D.F., Maechling, C.R., and Zare, R.N. (1996) Search for past life on Mars: Possible relic biogenic activity in Martian meteorite ALH 84001. Science, 273, 924–930.

Pimenta, M.A., Dresselhaus, G., Dresselhaus, M.S., Cancado, L.G., Jorio, A., and Saito, R. (2007) Studying disorder in graphite-based systems by Raman spectroscopy. Physical Chemistry Chemical Physics, 9, 1276–1291.

Shi, L., Lin, H., Bao, K., Cao, J., and Qian, Y. (2010) Controlled growth of carbon spheres through the Mg-reduction route. Nanoscale Research Letters, 5, 20–24.

Smith, P.P.K. and Buseck, P.R. (1981) Graphitic carbon in the Allende meteorite: a microstructural study. Science, 212, 322–324.

Steele, A., Goddard, D.T., Stapleton, D., Toporski, J.K.W., Peters, V., Bassinger, V., Sharples, G., Wynn-Williams, D.D., and McKay, D.S. (2000) Investigations into an unknown organism on the Martian meteorite Allan Hills 84001. Meteoritics & Planetary Science, 35, 237–241.

Steele, A., Fries, M.D., Amundsen, H.E.F., Mysen, B.O., Fogel, M.L., Schweizer, M., and Boctor, N.Z. (2007) Comprehensive imaging and Raman spectroscopy of carbonate globules from Martian meteorite ALH 84001 and a terrestrial analogue from Svalbard. Meteoritics & Planetary Science, 42, 1549–1566.

Steele, A., McCubbin, F.M., Fries, M., Glamoclija, M., Kater, L., and Nekvasil, H. (2010) Graphite in an Apollo 17 impact melt breccia. Science, 329, 51–51.

Talyzin, A.V., Szabo, T., Dekany, I., Langenhorst, F., Sokolov, P.S., and Solozhenko, V.L. (2009) Nanocarbons by high-temperature decomposition of graphite oxide at various pressures. Journal of Physical Chemistry C, 113, 11279–11284.

Tan, Z., Chihara, H., Koike, C., Abe, H., Kanecko, K., Sato, K., and Ohara, S. (2010) Interstellar analogs from defective carbon nanostructures account for interstellar extinction. The Astronomical Journal, 140, 1456–1460.

Treiman, A.H. (2003) Submicron magnetite grains and carbon compounds in Martian meteorite ALH 84001: Inorganic, abiotic formation by shock and thermal metamorphism. Astrobiology, 3, 369–392.

Treiman, A.H. and Essene, E.J. (2011) Chemical composition of magnetite in Martian meteorite ALH 84001: Revised appraisal from thermochemistry of phases in Fe-Mg-C-O. Geochimica et Cosmochimica Acta, 75, 5324–5335.

Treiman, A.H., Amundsen, H.E.F., Blake, D.F., and Bunch, T. (2002) Hydrothermal origin for carbonate globules in Martian meteorite ALH 84001: a terrestrial analogue from Spitsbergen (Norway). Earth and Planetary Science Letters, 204, 323–332.

van Zuilen, M.A., Lepland, A., Teranes, J., Finarelli, J., Wahlen, M., and Arrhenius, G. (2003) Graphite and carbonates in the 3.8 Ga old Isua Supracrustal Belt, southern West Greenland. Precambrian Research, 126, 331–348.

Yang, H.F., Yan, Y., Liu, Y., Zhang, F.Q., Zhang, R.Y., Meng, Y., Li, M., Xie, S.H., Tu, B., and Zhao, D.Y. (2004) A simple melt impregnation method to synthesize ordered mesoporous carbon and carbon nanofiber bundles with graphitized structure from pitches. Journal of Physical Chemistry B, 108, 17320–17328.

Manuscript received February 28, 2012
Manuscript accepted April 2, 2012
Manuscript handled by Ian Swainson